

Thermal Expansion Coefficients of Low-K Dielectric Films from Fourier Analysis of X-ray Reflectivity

C.E. Bouldin, W.E. Wallace, G.W. Lynn*, S.C. Roth and W.L. Wu
National Institute of Standards and Technology, Gaithersburg MD, 20899

**Also, Dept. of Chemistry, University of Tennessee, Knoxville*

(December 9, 1999)

Abstract

We determine the thermal expansion coefficient of a fluorinated polyimide low-k dielectric film using Fourier analysis of x-ray reflectivity data. The approach is similar to that used in Fourier analysis of x-ray absorption fine structure. The analysis compares two similar samples, or the same sample as an external parameter is varied, and determines the change in film thickness. The analysis process is very accurate, and depends on no assumed model. We determine a thermal expansion coefficient of $55 \pm 9 \times 10^{-6} \text{K}^{-1}$ using this approach.

61.10Kw,77.55tf,65.70.ty,06.30.Bp,02.30.Nw,68.60.Dv

I. INTRODUCTION

High-density integrated circuits use multilevel interconnects to increase device density. By using vertical stacking of conductive layers separated by dielectric films, better use is made of silicon area, preserving wafer space for active devices. As device density is scaled into the $0.18\ \mu\text{m}$ regime, a transition to low-k dielectrics becomes increasingly attractive, due to lower line-to-line capacitance, reduced cross-talk and lower power dissipation. These new interlayer dielectrics must meet stringent materials requirements, and these properties must be uniform across a wafer area and precisely controlled as dielectric layers are reduced to submicron dimensions. Thin film dielectrics can be very different than their bulk counterparts, so materials properties must be made on actual devices, or at least on isolated films that are prepared as they will ultimately be used in the film stack [1–3]. In particular, the thermal expansion coefficient (TEC) of the dielectric layers must be measured since electronic devices run at elevated and variable temperatures, causing thermal stresses that are a leading cause of chip failures. The need for precision *in situ* TEC measurements has driven the development of new measurement techniques. For thicknesses greater than $\sim 2\ \mu\text{m}$, precision TEC measurements have been made using capacitance measurements [4]. However, below this thickness and especially for silicon substrates, other methods are required. In this paper, we show that x-ray reflectivity (XRR) can be used to accurately measure the thickness and TEC of low-k dielectric films on silicon substrates.

X-ray reflectivity is now used as a routine characterization tool of thin films [5]. In the thickness range of $\sim (50 - 10,000)\ \text{\AA}$, XRR can be used to determine film thicknesses, densities and interface roughnesses. Film stacks on a substrate give rise to oscillations in the XRR above the critical angle of the films, with the frequencies of the oscillations determined by the thicknesses of the layers in the film stack. The usual approach for extracting these parameters is to start with an assumed structural model and then use non-linear least squares methods to refine a set of structural parameters to fit the full reflectivity curve [6]. In most cases this works well, but it is subject to some pitfalls because of the assumed

starting point of the model and because there can be a large number of correlated parameters in the model. In simple systems, consisting of one or two layers on a substrate, Fourier analysis methods have been applied to the reflectivity data [7,8]. Fourier methods allow a separate determination of each thickness in a film stack so long as the frequencies are resolvable in a Fourier transform. However, the Fourier methods used to date suffer from several drawbacks. The accuracy of the thicknesses determined by the Fourier transform method has been limited by the measurement of the position of a sharp peak in the Fourier transform magnitude. We use a band-pass limited inverse Fourier transform and measure the phase variation of single Fourier component in Q-space to determine accurate thickness and thickness changes between two films, an analysis method that is similar to that used in x-ray absorption spectroscopy [9]. Using this approach we are able to measure changes in film thickness of $9.0 \pm 1.5 \text{ \AA}$ in films that are $\sim 6100 \text{ \AA}$ thick. We also show that in high quality films, we are able to use higher harmonics in the reflectivity data as an accuracy check on the thickness determination. By measuring very small changes in low-k dielectric film thicknesses with temperature we are able to determine accurate thermal expansion coefficients using only two data points separated by just 25°C .

The approach used here to determine thermal expansion coefficients is a differential analysis that is applicable in two broad cases of practical interest. First, thin films are now used in a variety of technological applications where the same structures must be produced many times through careful process control. In these films the interest is in small departures from an accurately known baseline structure rather than a determination of an unknown structure *ab initio*. Second, we are often interested in the structural variation caused by an extrinsic parameter, such as temperature, pressure or an applied field (the extrinsic parameter can also be a systematic variation in a single processing parameter). In these cases the analysis shown here will produce accurate results; we illustrate this by a measurement of the thermal expansion coefficient of a fluorinated polyimide low-k film on silicon. In addition to determining thickness changes, we show that Fourier filtering the XRR data can determine the absolute film thicknesses; this is a generalization of the well-known approach

of using the anti-node locations in the XRR [10]. By Fourier filtering the data, we extend that method so that it can handle multi-layer film stacks and improve the accuracy of the thickness determination.

II. EXPERIMENT

The film studied here was a fluorinated polyimide film (FLARE) grown by Allied Signal. The film is a highly crosslinked poly (ether ether ketone) based polymer cured at 425 °C, with a dielectric constant of 2.80 and a glass transition temperature of 450 °C [11,12].

The XRR measurements were made with a Philips model XPERT MRD reflectometer [12]. Only specular reflectivity was collected, with the grazing incident angle equal to the detector angle. The angle ranged from (0.011 to 14) mrad. The XRR measurements were conducted in a $\theta - 2\theta$ configuration with a fine focus 2 KW copper x-ray tube. The incident beam was conditioned with a four-bounce germanium (220) monochromator. Before the detector, the beam was further conditioned with a three-bounce germanium (220) channel cut crystal. This configuration results in a copper $K_{\alpha 1}$ beam with a fractional wavelength spread of $\Delta\lambda/\lambda = 1.3 \times 10^{-4}$ and an angular divergence of 5.8×10^{-5} mrad. The motion of the goniometer is controlled by a closed-loop active servo system with an angular reproducibility of 1.7×10^{-3} mrad. These high precision settings in both the x-ray optics and the goniometer control are necessary to detect the very narrowly spaced interference fringes from films on the order of one micrometer thick. Measurements were made at 50 and 75 °C. The sample was inside a vacuum chamber equipped with thin Be windows to admit the incident and reflected x-ray beams. Pressure was less than 67 mPa to avoid oxidation. Temperature measurements at 50 ± 0.5 °C and 75 ± 0.5 °C were interleaved with coolings to room temperature to insure that no film changes took place at elevated temperatures.

III. X-RAY REFLECTIVITY

For x-rays, the index of refraction of a material is given by

$$n = 1 - \frac{N}{2\pi} r_0 \lambda^2 \sum_j \frac{\rho_j}{A_j} f_j \quad (1)$$

where N is Avogadro's number, r_0 is the classical electron radius, $\lambda = hc/E$ is the x-ray wavelength, the sum is over the elements in the material, the ρ_j , A_j , and f_j are the density, atomic mass and form factors of the j th element. In general, $f_j = f_{0j} + f'_j + i f''_j$, where f_{0j} is the Thomson scattering and f'_j and f''_j are the real and imaginary anomalous dispersion corrections. Far from absorption edges of the elements in the material the f'_j and f''_j may be ignored and $f_0 \approx Z$ in the near-forward scattering used in x-ray reflectivity. Including the anomalous dispersion corrections, the index of refraction is

$$n = 1 - \delta - i\beta \quad (2)$$

where

$$\begin{aligned} \beta &= \frac{N}{2\pi} r_0 \lambda^2 \sum_j \frac{\rho_j}{A_j} f''_j = \frac{\mu\lambda}{4\pi} \\ \delta &= \frac{N}{2\pi} r_0 \lambda^2 \sum_j \frac{\rho_j}{A_j} (f'_j + Z_j) \end{aligned} \quad (3)$$

Two useful simplifications can be made. As mentioned above, the anomalous dispersion correction to f' can be neglected since the x-ray energy is not near any absorption edges. This makes calculation of the index simply a matter of knowing the electron density, and this parameter is available from the measurement of the critical angle. Also, the index of refraction is virtually independent of temperature, because the x-rays are most strongly scattered by electrons that have binding energies that are very large compared with the measurement temperatures.

In the simplest case of a bare substrate, the x-rays are totally reflected at angles less than $\theta_c = \sqrt{2\delta}$. The next possible case is a three layer system of air-film-substrate, in which interference effects are possible between the x-rays reflected at the air-film and film-substrate interfaces, giving rise to oscillations in the XRR. When the reflectivity is small, the XRR can be written as [7,8]

$$R = \frac{F_{1,2}^2 + F_{2,3}^2 - 2F_{1,2}F_{2,3} \cos(\gamma d)}{1 - F_{1,2}^2 - F_{2,3}^2 + F_{1,2}^2 F_{2,3}^2}$$

$$= A + B \cos(\gamma d) \tag{4}$$

where $\gamma = (4\pi/\lambda)\sqrt{\theta^2 - \theta_c^2}$, $F_{j-1,j}$ are the Fresnel coefficients at the interface of the $j - 1$ th and j th layers, θ and θ_c are the angle of x-ray incidence and the critical angle, λ is the x-ray wavelength and d is the film thickness.

Therefore, at angles greater than the critical angle, the thickness of a film may be determined by the peak positions in a Fourier transform with respect to γ [7,8]. We extend this approach in two ways. After a forward Fourier transform, we take a band-pass selected inverse Fast Fourier Transform (FFT) to isolate a single frequency in the data, and then extract the phase of the cosine oscillation as $\phi = \gamma d = \arctan(\Im(FFT)/\Re(FFT))$. When plotted versus γ , this results in a straight line with a slope of d , which determines the absolute film thickness. Analyzing the phase of the cosine oscillation versus γ avoids the problem of precisely fixing the position of a sharp peak in real space. We plot differences of $\Delta\phi = \gamma\Delta d$ versus γ . In this case, the slope of the linear plot gives the *change* in the film thickness between two measurements. As in x-ray absorption analysis, this differential method tends to cancel any systematic errors in the data and minimizes Fourier filtering errors.

Extracting the phase of the cosine oscillations is equivalent to plotting anti-nodes in the reflectivity data versus γ [10], but improves upon that approach in three ways. First, the phase of the cosine oscillation is determined as a continuous variable, not just sampled at intervals of π . Second, the band-pass filtering allows multi-layer film stacks to be analyzed because the frequencies can be separated in the Fourier transform. Third, the band-pass filter removes noise from the data, giving more accurate results.

The Fourier analysis was done using the program Igor [13,12]. The oscillatory part of the XRR was isolated by fitting the full reflectivity with a smoothing spline. This is a spline with sufficient degrees of freedom to exactly reproduce the data, but a constraint on the second derivative causes the spline to follow a smooth approximation to the data. The smoothness parameter was varied and set to a value just below the point that would

allow the spline to contain oscillations of the same frequency as the cosine oscillations from the film scattering. Once the oscillatory term was isolated, it was multiplied by a Hanning window function before the first Fourier transform. A square window function was used for the inverse Fourier transform.

We now illustrate this methodology by determining the film thickness, and film thickness change with temperature for a $\sim 6100 \text{ \AA}$ low-k dielectric film on a silicon substrate. Because we are able to measure film thickness changes of just a few angstroms, we are able to determine the TEC of this thin film *in situ* on a silicon substrate.

IV. DATA AND RESULTS

The XRR data for the low-k dielectric film at 50°C are shown in Fig. 1. They have been corrected for “footprint” effects and are shown on a linear scale, plotted against sample angle θ . On this scale, the XRR data at 75°C are indistinguishable.

In Fig. 1, the low-k dielectric film θ_c is at $\sim 3 \text{ mrad}$, and the silicon θ_c is at about 4 mrad . Between the two critical angles there is a wave-guiding region in which strong reflection takes place from the top and bottom of the low-k dielectric film. Above the silicon critical angle the reflectivity falls quickly and the oscillatory structure is predominantly due to single-scattering interference between x-rays reflected from the top of the low-k dielectric film and the film-silicon interface.

To clearly demonstrate the analysis procedure, we constructed simulated data using MLAYER [6] and applied the Fourier analysis to both the real and simulated data. The simulated data sets were constructed to be low-k dielectric films on silicon substrates with thicknesses of 6475 \AA and 6470 \AA , and random noise was added to the simulated data until the signal-to-noise ratio approximated that of the real data. No interface roughness was used in the simulations. In Figs. 2 and 3 we show the results of the Fourier analysis of simulated (Fig. 2) and real data (Fig. 3). In the upper panel of these figures we show XRR plotted versus γ , and the phase difference $\Delta\phi$ for the fundamental and first harmonic peaks

in the Fourier transform. In the lower panel we show the Fourier transform magnitudes. In both figures we see, in addition to a peak that corresponds to the film thickness, a series of 3 harmonics. These are just the Fourier components of an expansion of a step function in the charge density, and they are visible because of the long range of the data and the low roughness at the interfaces. The peaks decrease in size faster than the expected rate for Fourier expansion coefficients of a square wave because of the finite data cutoff in Q and roughness of the interfaces. In the inset in Fig. 3, note that the second and third harmonics of the 75 °C data are smaller than at 50 °C, as expected, because the higher temperature decreases the interface abruptness.

Absolute film thicknesses are determined in a similar manner, except that the analysis uses a plot of ϕ , rather than $\Delta\phi$ versus γ . The ϕ plots are shown in Fig. 4. Since the total phase undergoes a change of about 400 radians, the ϕ plots are shown as phase residuals after subtraction of the best straight line fit. The top panel shows the phase residual of the 50 °C data after subtracting a thickness of 6102.0 Å. The bottom panel shows a similar plot for the 75 °C data after subtracting a thickness of 6111.4 Å. Since the phase residuals are very close to zero, this shows that the film thickness changes from $D(50\text{ °C}) = 6102.0 \pm 1.5$ Å to $D(75\text{ °C}) = 6111.4 \pm 1.8$ Å. Using the difference between the absolute thickness measurements gives a thickness change of 9.4 ± 2.6 Å, consistent with the determination made from the phase difference.

V. DISCUSSION

Fourier analysis of XRR data makes very accurate determinations of absolute film thicknesses and temperature-dependent thickness changes. The approach used here for determining a TEC is also applicable in any case where a comparison is made between reflectivity spectra that are similar. In practical terms, there are two cases of interest: (1) making an accurate determination of the film thickness in ostensibly identical samples, such as in quality control of thin-film materials fabricated for technological applications, and (2) in

determining layer thickness changes when an external parameter, such as temperature, is changed.

The Fourier analysis presented here differs from earlier work in several ways. First, both forward and inverse Fourier transforms are used. This allows separate determinations of layer thicknesses in multi-layer thin film stacks. We band-pass filter peaks in the forward Fourier transform and use the Q-space variation of single frequency to measure the corresponding layer thickness. This approach is much easier than picking off the exact position of a sharp peak in R-space. The inverse Fourier transform method is a generalization of the well-known approach of counting anti-node spacings [10] in a reflectivity curve, but improves on the anti-node plot in three ways: (1) the phase of the cosine oscillation in the XRR is treated as a continuous variable, not just determined at discrete points, (2) multi-layer films can be easily handled if the frequencies corresponding to each layer are separable in the Fourier transform, (3) the signal-to-noise ratio is improved by the Fourier band-pass filter.

This analysis method has been illustrated here by a study of the thermal expansion of a low-k dielectric film on a silicon substrate. We determine a thicknesses of $D(50^\circ\text{C}) = 6102.0 \pm 1.5 \text{ \AA}$ and $D(75^\circ\text{C}) = 6111.4 \pm 1.8 \text{ \AA}$, giving a thickness change of 9.4 \AA , and from the phase difference we determine a thickness change of $9.0 \pm 1.5 \text{ \AA}$; both results give a thermal expansion coefficient of $55 \pm 9 \times 10^{-6} \text{K}^{-1}$. Because of the perfection of the samples and the abrupt film-silicon interface, we are able to observe the fundamental and 3 harmonics in the XRR oscillations. Analysis of the first harmonic gives a film thickness change of $8.6 \pm 1.5 \text{ \AA}$, consistent with the change measured using the fundamental.

XRR is shown to measure film thickness changes with sufficient accuracy to determine TECs that are $\geq 10 \times 10^{-6}$. The TEC measurements can be made *in situ* on films that are 100-1000 nm thick on silicon substrates. Thus, XRR provides TEC measurements that can span much of the film thickness range below the limit of $\sim 2\mu\text{m}$ that can be achieved with capacitive measurements [4]. The films need not be free-standing and silicon substrates are easily accommodated. Previous capacitive measurements have given a TEC of $\sim 100 \times 10^{-6} \text{K}^{-1}$ for thick polyimide films similar to the FLARE sample measured here, in reasonable

agreement with our results. XRR determinations of TEC are non-contacting and non-destructive, but require a sample area of the order of 1cm^2 and extreme wafer-flatness. In the present experimental arrangement only the perpendicular TEC is measured.

The accurate film thickness and TEC measurements are possible due to the highly perfect sample with smooth interfaces and low absorption. Using forward and inverse Fourier transforms we accurately measure the phase shift in the oscillatory term in the XRR and obtain precise thickness measurements. Analysis of neutron reflectivity data would proceed in exactly the same manner and might prove useful since neutrons have much lower absorption than 1.54 \AA x-rays, allowing TEC measurements in higher-Z films. We observed 3 harmonics in the Fourier transform of the XRR. These harmonics are simply the next terms in the Fourier expansion of the step function in the electron density due to the film. The falloff of these harmonics with temperature shows that they can give information about the interface roughness. The higher harmonics fall off in intensity more quickly than expected for the Fourier expansion of a step function because of interface roughness, which is larger in the 75°C data, and because the information about the sharper features in the electron density is contained in the higher harmonics. Sharp features in the electron density are observable only at higher values of γ_{min} , but the $\sim 1/\theta^4$ decay of the reflectivity imposes a hard value of γ_{max} so that the data range of each successive harmonic is squeezed into shorter ranges in γ , decreasing the size of the harmonic peaks in the Fourier transform. In nearly ideal samples, such as low-Z dielectric films on silicon, the data range and noise level of our measurement suggests that the ultimate sensitivity of XRR for measuring TEC is about $\sim 10^{-5}\text{K}^{-1}$.

We thank N. Rutherford of Allied Signal for providing the FLARE sample used in this study.

VI. FIGURES

FIGURES

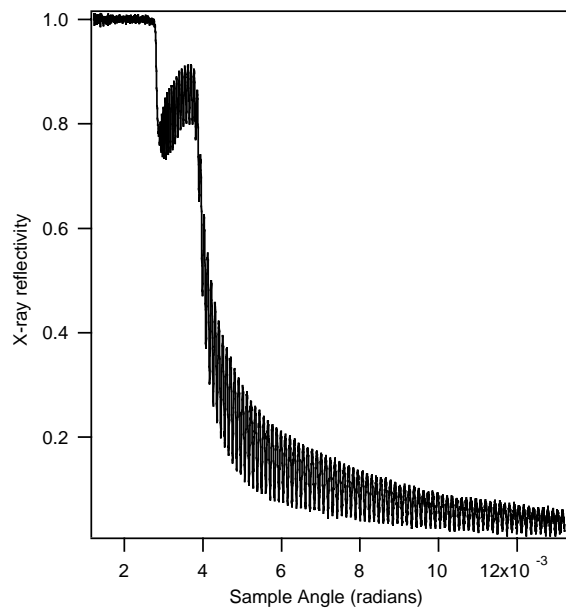


FIG. 1. X-ray reflectivity from ~ 6100 Å low-k dielectric film on silicon. The data have been footprint corrected below the film critical angle.

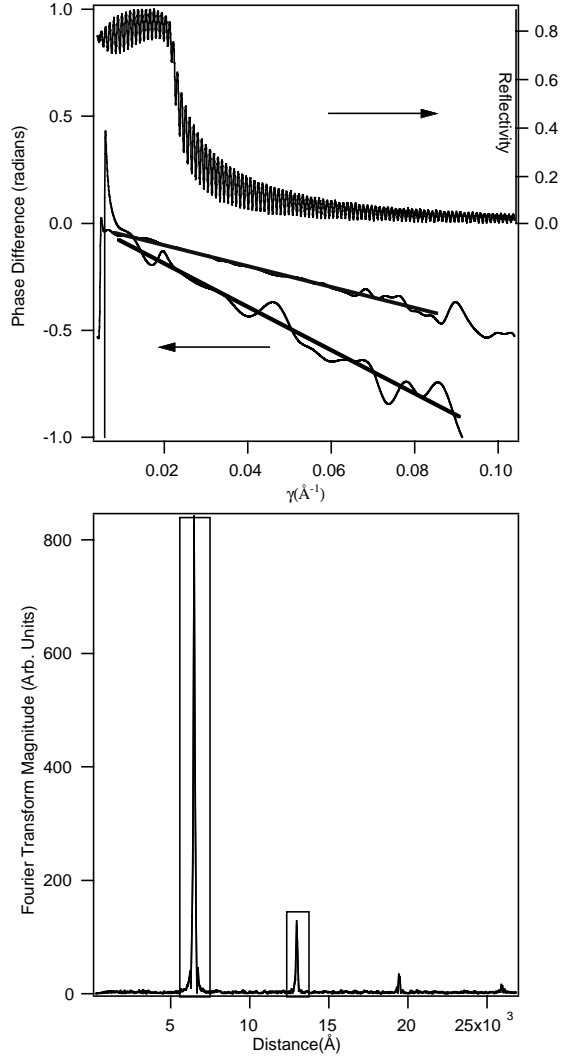


FIG. 2. Simulated X-ray reflectivity from 6470 Å and 6475 Å low-k dielectric films on silicon plotted against q , as described in the text. Top panel shows the raw data above the silicon θ_c and the $\Delta\phi$ of the first and second peaks in the Fourier transform. The phase differences from the two peaks imply a thickness change of 4.8 ± 0.5 Å and 5.6 ± 0.8 Å, respectively. Since the simulated data were constructed with $\Delta d \equiv 5.0$ Å, this gives a measure of how well the analysis works. Lower panel shows the Fourier transform magnitudes of both data sets. The Fourier band-pass filters used are shown as boxes around the first and second peaks.

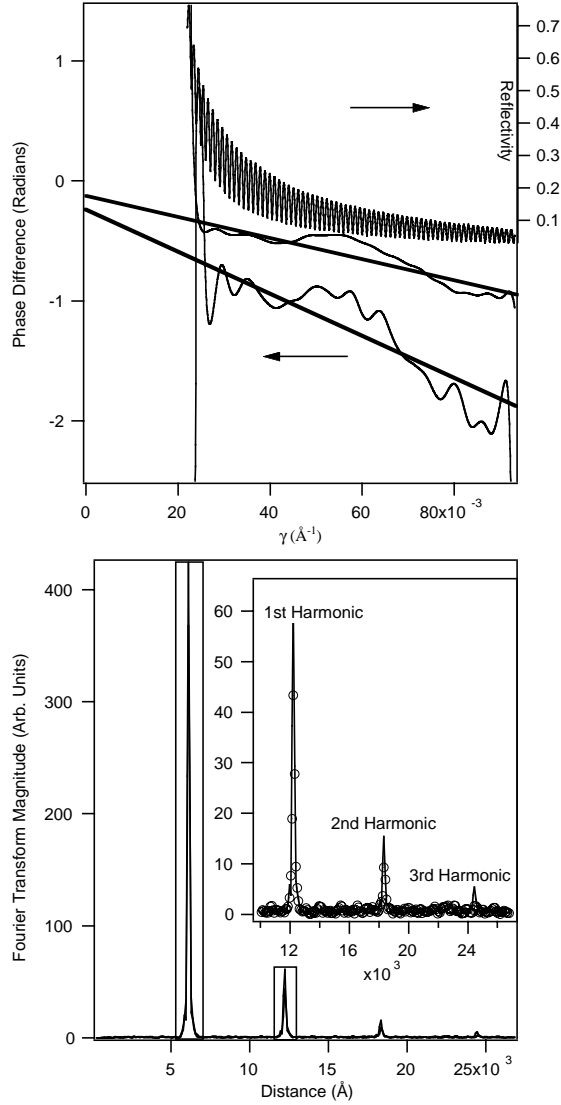


FIG. 3. X-ray reflectivity from 6100 Å low-k dielectric films at 50 °C and 75 °C, on silicon plotted against γ , as described in the text. Top panel shows the raw data above the silicon θ_c and the $\Delta\phi$ of the first and second peaks in the Fourier transform. The phase differences from the two peaks imply a thickness change of $9.0 \pm 1.5\text{Å}$ and $8.6 \pm 1.5\text{Å}$, respectively. Lower panel shows the Fourier transform magnitudes of both data sets. The Fourier band-pass filters used are shown as boxes around the first and second peaks. The inset in the lower figure shows that the higher harmonic peaks are suppressed by loss of interface sharpness at 75 °C.

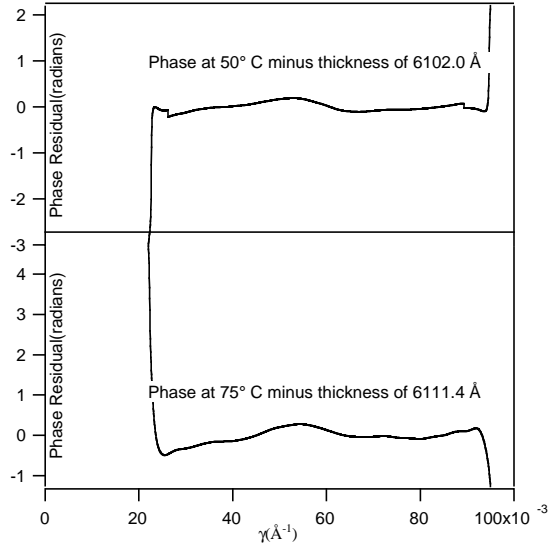


FIG. 4. Top panel, phase residual of the cosine oscillation $\phi = \gamma d$ in the 50°C after subtracting a linear fit with $D(50^\circ\text{C}) = 6102.0 \pm 1.5 \text{ \AA}$. Bottom panel, phase residual of the cosine oscillation $\phi = \gamma d$ in the 50°C after subtracting a linear fit with $D(75^\circ\text{C}) = 6111.4 \pm 1.8 \text{ \AA}$.

REFERENCES

- [1] H. V. Z. W. Wu and W. Orts, *Macromolecules* **28**, 771 (1995).
- [2] T. P. P.S. Ho and J. Leau, *J. Phys. Chem. Solids* **55**, 1154 (1994).
- [3] R. J. J.L. Keddie and R. Cory, *Europhys. Lett.* **27**, 59 (1994).
- [4] C. Synder and F. Mopsik, *RSI* **69**, 3899 (1998).
- [5] B. Lengeler, *Adv. in X-ray Anal.* **35**, 127 (1992).
- [6] J. F. Anker and C. F. Majkrzak, *SPIE, Neutron Optical Devices and Applications* **1738**, 260 (1992).
- [7] K. Sakurai and A. Itda, *Jap. J. Appl. Phys.* **31**, L113 (1992).
- [8] K. Sakurai and A. Itda, *Phys. Rev. B* **35**, 813 (1992).
- [9] G. Bunker, *Nuc. Inst. Meth.* **207**, 437 (1983).
- [10] Armin Segmüller, *Thin Solid Films* **18**, 287 (1973).
- [11] N. P. Hacker, *MRS Bulletin* **22**, 33 (1997).
- [12] Certain commercial equipment, instruments, or materials are identified in this paper in order to adequately specify the experimental procedure. Such identification does not imply recommendation or endorsement by the National Institute of Standards and Technology, nor does it imply that the materials or equipment identified are necessarily the best available for the purpose.
- [13] See www.wavemetrics.com.